



# An electrochemical aptasensor for $\Delta^9$ -tetrahydrocannabinol detection in saliva on a microfluidic platform

László Kékedy-Nagy<sup>a,b</sup>, James M. Perry<sup>b,c</sup>, Samuel R. Little<sup>a,b</sup>, Oriol Y. Llorens<sup>a,b</sup>, Steve.C. C. Shih<sup>a,b,c,\*</sup>

<sup>a</sup> Department of Electrical and Computer Engineering, Concordia University, 1455 de Maisonneuve Blvd West, Montreal, Quebec, H3G1M8, Canada

<sup>b</sup> Centre for Applied Synthetic Biology, Concordia University, 7141 Sherbrooke St. West, Montreal, Quebec, H4B1R6, Canada

<sup>c</sup> Department of Biology, Concordia University, 7141 Sherbrooke St. West, Montreal, Quebec, H4B1R6, Canada

## ARTICLE INFO

### Keywords:

Electrochemistry  
Tetrahydrocannabinol  
Methylene blue  
Aptasensor  
Microfluidics  
Saliva

## ABSTRACT

We present a novel “on-off”, cost-effective, rapid electrochemical aptasensor combined with a microfluidics cartridge system for the detection of  $\Delta^9$ -THC ( $\Delta^9$ -tetrahydrocannabinol) in human saliva *via* differential pulse voltammetry. The assay relied on the competitive binding between the  $\Delta^9$ -THC and a soluble redox indicator methylene blue, using an aptamer selected *via* FRELEX. We found that the aptasensor can detect 1 nM of  $\Delta^9$ -THC in PBS in a three-electrode cell system, while the sensitivity and both the dissociation constant ( $K_d$ ) and association constant ( $K_b$ ) were dependent on the aptamer density. The aptamer also showed great affinity towards  $\Delta^9$ -THC when tested against cannabidiol and cannabidiol. The same limit of detection of 1 nM in PBS was achieved in small volume samples (~60  $\mu$ L) using the aptamer-modified gold screen-printed electrodes combined with the microfluidic cartridge setup, however, the presence of 10% raw human saliva had a negative effect which manifested in a 10-fold increase in the LOD due to interfering elements. Filtering the saliva, improved the tested volume to 50% and the LOD to 5 nM of  $\Delta^9$ -THC which is lower than the concentrations associated with impairment (6.5–32 nM). The aptasensor showed a good storage capability up to 3 days, however, the reusability significantly dropped from 10 cycles (freshly prepared) to 5 cycles. The results clearly demonstrate the feasibility of the aptasensor platform with the microfluidics chamber towards a point-of-care testing application for the detection of  $\Delta^9$ -THC in saliva.

## 1. Introduction

The *Cannabis sativa* plant produces over 85 unique compounds known as cannabinoids which include cannabidiol (CBD), cannabinol (CBN) and  $\Delta^9$ -tetrahydrocannabinol ( $\Delta^9$ -THC). Cannabis products are widely used as therapeutic and recreational drugs (Grotenhermen, 2003; Vemuri and Makriyannis, 2015), and in particular, the psychoactive effects of  $\Delta^9$ -THC makes it common target for drug screening in medical, athletic and law enforcement contexts (Connors et al., 2020; Johnson et al., 2022; Kennedy, 2022; Saugy et al., 2006). Since  $\Delta^9$ -THC impairs psychomotor function, cannabis use is strictly prohibited before operating a motor vehicle or heavy machinery. This presents a challenge to improve the access and efficacy of road-side and job site drug testing

(Darzi and Garg, 2020; Klimuntowski et al., 2020). Cannabis use also has a relationship with mental health, where there is strong evidence supporting a link between cannabis use in adolescence and the development of Schizophreniform psychoses (Degenhardt et al., 2007; Hall and Degenhardt, 2008) as well as acute  $\Delta^9$ -THC use leading to psychosis-like symptoms such as paranoia, anxiety or insomnia. A recent study characterizing self-reporting in clinical settings found only 12.5% of positively-tested subjects admitted to cannabis use within 72 h of arrival, therefore rapid  $\Delta^9$ -THC testing in a healthcare setting is needed to accurately assess patients who may suffer from mental health disorders (Khalili et al., 2021).

Monitoring cannabis use in hospitals or at sporting events mainly rely on gas- or liquid chromatography-mass spectrometry of prepared

**Abbreviations:**  $\Delta^9$ -THC,  $\Delta^9$ -tetrahydrocannabinol; CV, cyclic voltammetry; DPV, differential pulse voltammetry; CBN, cannabinol; CBD, cannabidiol; MB, methylene blue; LOD, limit of detection; SPE, screen-printed electrodes.

\* Corresponding author. Department of Electrical and Computer Engineering, Concordia University, 1455 de Maisonneuve Blvd West, Montreal, Quebec, H3G1M8, Canada.

E-mail address: [steve.shih@concordia.ca](mailto:steve.shih@concordia.ca) (Steve.C.C. Shih).

<https://doi.org/10.1016/j.bios.2022.114998>

Received 19 October 2022; Received in revised form 21 November 2022; Accepted 6 December 2022

Available online 8 December 2022

0956-5663/© 2022 Elsevier B.V. All rights reserved.

blood or urine samples (Klimuntowski et al., 2020). This process is expensive, time consuming and cannot be performed outside of a laboratory setting (Johnson et al., 2022). Moreover, individuals can test positive for up to 10 days after psychoactive effects have been resolved, due to the body's slow process of releasing accumulated  $\Delta^9$ -THC from fat tissue (Connors et al., 2020; Howard and Osborne, 2020). Roadside methods such as the field-sobriety test (Papafotiou et al., 2005) or colorimetric tests (Johnson et al., 2022), are considered highly subjective or unreliable.

Recently, there have been breath analysis tests paired with various analytical techniques such as fluorescence (Hound Labs), microfluidics (Cannabix Technologies), field asymmetric mobility spectrometry (FAIMS, Cannabix Technologies), and s-SWCNTs chemiresistors (Star Labs), however, all of these systems have suboptimal sensitivities or selectivity (Johnson et al., 2022). The microfluidic-based artificial olfaction sensor's sensitivity requires further research to reliably detect the target level of 9.5 nM of  $\Delta^9$ -THC in breath (Mirzaei et al., 2020), while the FAIMS technology showed only a 65 ppb (~209 nM) detection of  $\Delta^9$ -THC, with limited portability (Paknahad et al. 2017, 2019). Chemiresistors-based sensors have promising sensitivity, however, the selectivity require further testing (Mirzaei et al., 2020). Yu et al. proposed a dynamic oral fluid test within 5 min for  $\Delta^9$ -THC detection down to 0.54 nM called EPOCH – relying on competitive immunoassay scheme. However, the complexity of the separate working modules and lack of sensitivity, makes this device less appealing for on-site detection (Yu et al., 2021b).

Alternatively, there has been work demonstrating electrochemical detection of small molecules using low-cost, highly sensitive, and portable devices – especially when integrated with microfluidics (De Rycke et al., 2020; Teymourian et al., 2020; Yu et al. 2021a, 2021b; Zheng et al., 2021). Several groups have achieved electrochemical detection by direct oxidization of  $\Delta^9$ -THC using a variety of different electrode materials, yet the formation of harmful by-products leads to electrode passivation, making direct oxidization ineffective (Balbino et al. 2012, 2016; Darzi and Garg, 2020; Goodwin et al., 2006; Majak et al., 2021; Nissim and Compton, 2015; Novak et al., 2013; Ortega et al., 2022; Renaud-Young et al., 2019; Zhang et al., 2021). However, using aptamer-based electrochemical detection can avoid the formation of harmful byproducts.

Aptamers are single-stranded nucleic acids which are evolved through *in vitro* selection called systematic evolution of ligands *via* exponential enrichment (SELEX), and can bind to virtually any target of interest (Liu et al., 2021; Yoo et al., 2020). To date, aptamers have been isolated for small-molecule targets, however, most have insufficient binding affinity or specificity for real-world applications (Stojanovic et al., 2001). Yu et al., (2021c) isolated a 47-nt long  $\Delta^9$ -THC-specific aptamer reporting a  $K_d$  of  $61 \pm 25$  nM, while quantifying the  $\Delta^9$ -THC in the 0.25–20  $\mu$ M range spectroscopically, which is higher than the 6.5–32 nM cut-off values required for detection in saliva (Gjerde and Verstraete, 2011; Vindenes et al., 2012).

In the present work, we show the first design and the electrochemical performance of the label-free 80-mer  $\Delta^9$ -THC specific aptamer, which was obtained *via* FRELEX (Penner, 2019) that utilizes analyte-interrupted oligo-oligo binding rather than resin immobilization. In our assay, we exploit the  $\Delta^9$ -THC's aptamer binding affinity which displaces the electrostatically bound redox indicator (methylene blue – MB) forming an electric wire which inhibits electron transfer (ET) at the working electrode. In addition, to move towards a rapid test, we show the integration of an “on-off” aptasensor with a microfluidic cartridge setup to rapidly detect  $\Delta^9$ -THC in saliva in a matter of minutes.

## 2. Materials and methods

### 2.1. Materials

Delta-9-tetrahydrocannabinol ( $\Delta^9$ -THC), cannabidiol (CBD),

methylene blue (MB), 6-mercapto-1-hexanol (MC<sub>6</sub>OH), Tris(2-carboxyethyl) phosphine hydrochloride (TCEP), potassium phosphate monobasic (KH<sub>2</sub>PO<sub>4</sub>), potassium phosphate dibasic (K<sub>2</sub>HPO<sub>4</sub>) and sodium chloride (NaCl) were all purchased from Sigma-Aldrich. Polylactic acid (PLA, blue – 2.85 mm dia.) filament was purchased from Innofil 3D (Mississauga, ON), and polydimethylsiloxane (PDMS - Sylgard 184, silicone elastomer base and curing agent) was purchased from The Dow Chemical Company (Midland, MI). The  $\Delta^9$ -THC specific binding aptamer (A-18, 80-base sequence) was designed by *in vitro* selection by using the FRELEX process (Penner, 2019) (see SI for details). The selected A-18 aptamer with a 5' C<sub>6</sub>-disulfide modification (HOC<sub>6</sub>-S-S-C<sub>6</sub>-5'-TGT CAC ATC TAC ACT GCT CGA AGG TCT TTC GTA TTT GCA TTC CTC TCT TCA TTT CGA GCA ATT CAG ACA GCG TTC CC-3') was synthesized by Metabion International AG, Martinsried, Germany. All solutions were prepared by using Milli-Q water (18 M $\Omega$ , Millipore, Bedford, MA, USA).

### 2.2. Aptamer modification of gold electrodes

Prior to modification, gold disk electrodes (CH Instruments, Austin, TX; diameter 1.6 mm) were cleaned as previously described (Ferafontova and Gothelf, 2009) and kept in absolute ethanol before modification, while gold screen-printed electrodes (SPE, PalmSens B.V., Houten, the Netherlands, diameter 2 mm) were cleaned according to Shanmugam et al., (2020) (see SI for details). The electrochemically-determined electrode surface area was obtained as previously described (Trasatti and Petrii, 1991) and were as follows:  $0.049 \pm 0.001$  cm<sup>2</sup> (disc) and  $0.058 \pm 0.004$  cm<sup>-2</sup> (SPE) (see SI for details). The aptamer surface coverage is reported for these surface areas. For aptamer modification, a mixture of 50 nM thiol-modified A-18 aptamer and 0.05 mM TCEP in 20 mM phosphate buffer solution/150 mM NaCl (20 mM PBS) at pH 7.0 was prepared and incubated for 1 h at room temperature (rt) for disulfide bond reduction. For preparation of self-assembled aptamer monolayers, a 10  $\mu$ L drop of the freshly prepared mixture was placed onto the clean gold electrode surface. The electrodes were covered with an Eppendorf vial and left overnight at rt. Next day the aptamer-modified electrodes were rinsed with PBS, and exposed to 10 mM MC<sub>6</sub>OH solution in the same buffer solution for 30 min. The aptamer-modified electrodes were subsequently stored in PBS until used.

### 2.3. Voltammetric characterization and analysis

Cyclic voltammetry (CV), differential pulse voltammetry (DPV) and electrochemical impedance spectroscopy (EIS) were carried out in a conventional three-electrode cell connected to a PalmSens 4 electrochemical system (PalmSens B.V., Houten, the Netherlands) equipped with PSTrace 5 (version 5.8) with the aptamer-modified gold electrodes where Ag/AgCl (3M KCl solution) and Pt wire was used as the reference and counter electrode, respectively. For SPE, a silver reference- and a gold counter electrode was used with a Sensit Smart (PalmSens B.V., Houten, the Netherlands) inserted in a smartphone and controlled *via* the Android app PStouch. In DPV, the modulation amplitude was 40 mV with a step potential of 10 mV and a scan rate of 20 mV s<sup>-1</sup>. The  $\Delta^9$ -THC binding was performed *in situ* by adding  $\Delta^9$ -THC directly in 20 mM PBS/1  $\mu$ M MB (pH 7.0), while for SPE, 60  $\mu$ L of the  $\Delta^9$ -THC/MB-containing PBS solutions were directly added on their surface followed by DPV. The EIS measurements were carried out using MC<sub>6</sub>OH-modified electrodes at polarization potential of -0.22 V in a frequency range of 0.1 Hz–1 MHz to with an amplitude of 5 mV vs. Ag/AgCl (3 M KCl). Unless otherwise stated, measurements were performed after 10 min incubation of the aptamer-modified electrodes in the  $\Delta^9$ -THC/MB-containing solutions, while the working solutions were not de-aerated. The MB surface coverage  $\Gamma_{\text{aptamer-MB}}$  was evaluated by integration of the MB cathodic peak area (see SI). All error bars show the standard deviations of measurements performed from three independent experiments.

## 2.4. Multistep analysis of $\Delta^9$ -THC in saliva samples with the EMMA-sense

Human saliva was collected after obtaining permission from four healthy adult volunteers (see participant characteristics, Table S1) into a Falcon 50 mL conical centrifuge tube (VWR International, Mississauga, ON) and were kept at 4 °C until analysis. For some experiments, saliva was filtered with Amicon Ultra-0.5 centrifugal filters from Millipore (Tullagreen, Ireland) by using an Eppendorf Centrifuge 5424 (Mississauga, ON) at 15,000 rpm for 30 min. For real-sample analysis, the saliva was spiked with 5 nM  $\Delta^9$ -THC before filtration. For  $\Delta^9$ -THC analysis, the aptamer-modified gold SPE was assembled with the homemade microfluidic chamber (see SI for additional experimental details and Video S1 assembly and operation of the device), while a 60  $\mu$ L aliquot of filtered or raw saliva diluted (50% or 90%) with 20 mM PBS/150 mM NaCl/1  $\mu$ M MB (pH 7.0) was pipetted into the inlet port of the EMMA-Sense and incubated for 1 min followed by DPV analysis. To test stability of the aptasensor, the devices were stored in a dry state at 4 °C for up to 7 days and DPV analysis was performed with spiked saliva on day 1, 3, and 7. The reusability of the sensor was explored by challenging the sensor with 5 nM  $\Delta^9$ -THC for 10 cycles by washing the sensor with PBS for 1 min and then adding the spiked saliva sample. The effectiveness of stability and regeneration protocol was verified by DPV on day 1, 3, and 7.

Supplementary data related to this article can be found at <https://doi.org/10.1016/j.bios.2022.114998>.

## 3. Results and discussion

### 3.1. Electroanalytical performance of the $\Delta^9$ -THC aptamer

*In vitro* selection of aptamers against  $\Delta^9$ -THC specific was achieved with FRELEX (Penner, 2019), where selection was performed for 9 selection rounds, using a library of oligonucleotides consisting of a random region of 40 nucleotides ( $10^{15}$  sequences). All oligos from selection round 6 to 9 were processed using next generation sequencing resulting in 54,177,178 analyzed sequences, with further analysis of the top twenty most abundant sequences (Table S2). These 20 aptamer frequencies all shared similar enrichment trajectories with successive selection rounds (Fig. S1). Next, we analyzed the specificity by comparing the enrichment in selection rounds 7, 8, and 9 against  $\Delta^9$ -THC versus CBD, resulting in aptamers A-7, A-8, and A-18 exhibiting the highest specificity (Fig. S2). Graphene oxide with fluorescently labeled aptamers were used to characterize aptamer- $\Delta^9$ -THC binding (Fig. S3), where the A-18 aptamer (see Fig. 1A) displayed the highest sensitivity towards  $\Delta^9$ -THC binding, therefore, it was used in the electroanalytical assay development.

Working with long sequence aptamers can be quite challenging due to their low sensitivity, non-specific binding, low affinity toward small molecules, and formation of unwanted secondary structures, therefore,

the success of the assay strongly depends on the design and the fine tuning of the working conditions (Liu et al., 2021; Yu et al., 2021a). In this work, a phenothiazine dye known as methylene blue (MB) was chosen as a soluble redox indicator, which offers different binding modes of interaction with nucleotides through electrostatic attraction, groove-binding, or intercalation between bases of dsDNA (Kelley et al., 1997). The positively charged MB typically undergoes a  $2e^-/H^+$  redox reaction at pH  $\sim$ 7, however, in certain conditions it can be a  $1e^-$  reaction (Campos et al., 2014; Kelley et al., 1997). The MB binding/dissociation constants in DNA films strongly depend on the ionic strength, for example, highly stable complexes were shown at lower ionic strength solutions (20 mM PBS) obtained for both d(GC)<sub>20</sub> and (dAT)<sub>25</sub> duplexes, with dissociation constants ( $K_d$ ) of 7.2 and 9.9  $\mu$ M, respectively (Kékedy-Nagy and Ferapontova, 2018), which can be further increased ( $K_d = 46 \mu$ M) when the complex is in 0.1 M NaCl (Nafisi et al., 2007). Using these conditions, we hypothesize the binding of  $\Delta^9$ -THC would disrupt the aptamer-mediated long-range electron transfer (ET) between the electrostatically attracted/intercalated MB and the gold surface, and therefore, an “on-off” signal is achieved, as shown by the schematic in Fig. 1B.

To test our hypothesis, representative DPVs were recorded with the aptamer/MC<sub>6</sub>OH-modified electrodes in 1  $\mu$ M MB solutions in the absence and presence of 5  $\mu$ M  $\Delta^9$ -THC, as shown in Fig. 2A. The results show a 2.8-fold decrease, with a positive potential shift from  $-218 \pm 3$  mV to  $-190 \pm 5$  mV, and an increase in the width of the DPV from 150 mV to 170 mV producing a robust “on-off” signaling aptasensor platform to measure  $\Delta^9$ -THC. The increase in width is likely due to the interruption of the highly directional ET through the aptamer of positively charged MB through the attachment of the uncharged  $\Delta^9$ -THC, making the ET more sluggish. In contrast, it is well known that highly directional ET is restricted by the sequence length, such that the MB located further from the electrode surface within the aptamer structure is considered electrochemically mute, and only the MB closer to the electrode is responsible for electrochemical signaling (Farjami et al., 2010; Jacobsen et al., 2009). Therefore, the  $\Delta^9$ -THC attaching closer to the electrode surface by replacing MB will have the biggest impact on the aptasensor platform, while the ones attaching further away from the surface will be less significant.

To have a better understanding about the surface behavior of the aptamer and their affinity towards  $\Delta^9$ -THC, the obtained signals were fitted to the appropriate adsorption isotherms, such as the Langmuir adsorption isotherm, that conveniently describes the affinity interaction between aptamers and their ligands (Kékedy-Nagy et al., 2016):

$$S = S_{\max} K_b [\Delta^9\text{-THC}] / (1 + K_b [\Delta^9\text{-THC}]) \quad (1)$$

and to the Scatchard model (Bueno and Davis, 2014):

$$S = S_{\max} [\Delta^9\text{-THC}] / (K_d + [\Delta^9\text{-THC}]) \quad (2)$$

where  $S$  is the change in the electrochemical signal,  $K_b$  is the constant

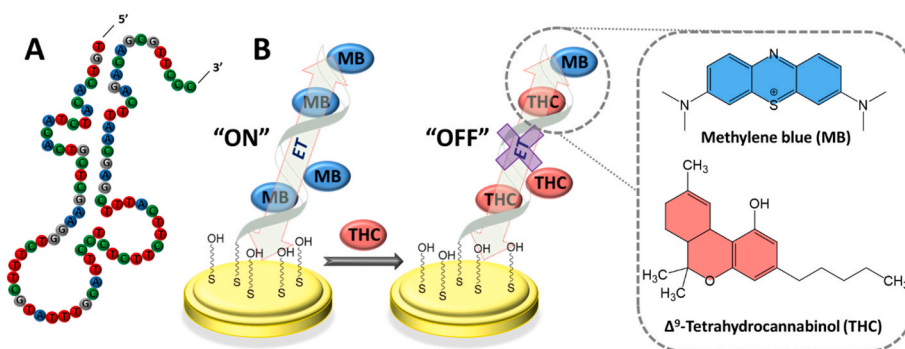


**Fig. 1.** (A) The chemical structure of the 80-mer DNA aptamer; (B) A general schematic representation of the electrochemical aptasensor assay in the presence of MB and  $\Delta^9$ -THC. Chemical structures of  $\Delta^9$ -tetrahydrocannabinol (THC) and methylene blue (MB) are shown in the highlighted dotted box.

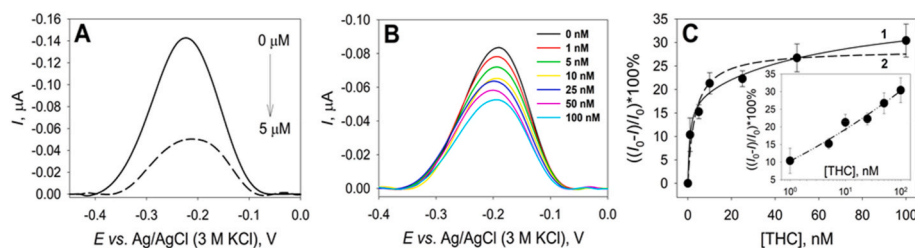


**Fig. 2.** DPVs recorded in 20 mM PBS/150 mM NaCl, pH 7.0 solution containing 1  $\mu\text{M}$  MB with the aptamer/MC<sub>6</sub>OH-modified electrode (A) before (solid line) and after (dashed line) incubation with 5  $\mu\text{M}$   $\Delta^9$ -THC; (B) Before (black line) and after (colored lines) the additions of 1, 5, 10, 25, 50, and 100 nM of  $\Delta^9$ -THC; and (C) DPV showing the changes in measured current (normalized to background levels) in the absence and the presence of various concentrations of  $\Delta^9$ -THC (1–100 nM), where data fitting was performed using (1) the Langmuir adsorption isotherm and (2) the Scatchard model to determine  $K_b$  and  $K_d$ .

Inset: the data normalized as logarithmic concentration. Surface density: (A)  $\Gamma_{\text{aptamer-MB}} = 1.8 \pm 0.3 \text{ pmol cm}^{-2}$ ; (B, C)  $\Gamma_{\text{aptamer-MB}} = 2.1 \pm 0.6 \text{ pmol cm}^{-2}$ . To correlate the current change and [THC], a logarithmic fit was used:  $(I_0 - I)/I_0 = ((I_0 - I)/I_0)_0 + a \cdot \log[\Delta^9\text{-THC}]$ , where  $a = 0.169$ .

reflecting the relation between the  $\Delta^9$ -THC binding/dissociation constants at the aptamer-modified surface,  $K_d$  is the dissociation constant, and  $[\Delta^9\text{-THC}]$  is the  $\Delta^9$ -THC concentration. Based on the fitting, the binding of  $\Delta^9$ -THC between 0 and 0.1  $\mu\text{M}$  yielded a  $K_b = 11 \pm 1.3$  and a significantly lower  $K_d = 0.1 \pm 0.01 \text{ }\mu\text{M}$  as described by the Scatchard model (Fig. S4B) (Bueno and Davis, 2014; Jarczewska et al., 2015) which suggests an increased apparent affinity towards the A-18 aptamer. Moreover, we observed a decrease in peak current for  $\Delta^9$ -THC concentrations between 0 and 0.1  $\mu\text{M}$ , which further suggest that the  $\Delta^9$ -THC is binding to the aptamer and not the electrode surface while showing potential sensitivity in the clinically relevant range (Fig. S4A).

Next, we assessed the performance of the aptasensor in the clinically relevant range (nM). As shown in Fig. 2B., we evaluated a dilutions series of  $\Delta^9$ -THC from 0 to 100 nM and observed similar fold-change ( $1.4 \pm 0.1$ ), peak shift ( $10 \pm 1 \text{ mV}$ ), and increase in width ( $23 \pm 5 \text{ mV}$ ) of the DPVs, following an “on-off” signaling scheme. However, electrodes with higher aptamer surface coverage produced larger currents (compared to the lower surface coverage; Fig. S5A), which we believe is caused by more MB binding to the aptamer due to increased numbers of aptamers. The calibration curve was constructed based on DPV responses, by plotting the relative current change  $(I_0 - I)/I_0$  with  $I_0$  being recorded in 1  $\mu\text{M}$  MB before the addition of  $\Delta^9$ -THC versus different  $\Delta^9$ -THC concentrations. The curves were fitted to a logarithmic function for the low surface coverage (Fig. 2C) as well as for the high-surface coverage which led to an improved sensitivity of the aptasensor system as shown by the calibration curves in Fig. S5B. The obtained  $K_b$  values were:  $4.9 \pm 1.3$  (low) and  $6.2 \pm 1.7$  (high), while the  $K_d$  values were  $2.1 \pm 0.8 \text{ nM}$  and  $0.5 \pm 0.1 \text{ nM}$  for low and high surface densities respectively, with a higher sensitivity towards  $\Delta^9$ -THC binding for the latter (Table 1). In addition, we were able to achieve a limit of detection (LOD) less than 1 nM  $\Delta^9$ -THC, which is suitable for the application of interest here (analysis of physiological relevant  $\Delta^9$ -THC levels in saliva (Renaud-Young et al., 2019), described below).

Analysis of the dependencies of the CV's  $I_p$  on the potential scan rate

**Table 1**

Surface density of aptamer-MB ( $\Gamma_{\text{aptamer-MB}}$  for 1  $\mu\text{M}$  MB concentration), dissociation constant ( $K_d$ ), association constant ( $K_b$ ), sensitivity and calculated/detected limit of detection ( $\text{LOD}_{\text{calc}}/\text{LOD}_{\text{det}}$ ) obtained with the aptamer/MC<sub>6</sub>OH-modified conventional gold disk-electrodes.

Aptamer coverage	$\Gamma_{\text{aptamer-MB}}$ , <sup>a</sup> pmol cm <sup>-2</sup>	$K_d$ , <sup>b</sup> nM	$K_b$ , <sup>c</sup>	Sensitivity <sup>c</sup> A-nM <sup>-1</sup>	$\text{LOD}_{\text{calc}}$ , <sup>d</sup> nM	$\text{LOD}_{\text{det}}$ , nM
Low	$2.1 \pm 0.8$	$2.1$	$4.9$	$(2.28 \pm 0.74)10^{-10}$	$0.41 \pm 0.03$	$1.0 \pm 0.0$
		$\pm 0.8$	$\pm 1.2$			
High	$5.3 \pm 0.9$	$0.5$	$6.2$	$(4.13 \pm 0.53)10^{-10}$	$0.13 \pm 0.01$	$1.0 \pm 0.0$
		$\pm 0.1$	$\pm 1.7$			

<sup>a</sup>from the CV peaks of MB according to Eq. (1); <sup>b</sup>, <sup>c</sup>from  $((I_0 - I)/I_0) \times 100\%$ ; <sup>c</sup>calculated from the slopes of the logarithmic plot; <sup>d</sup>calculated from the standard deviation ( $3\sigma$ ) of the background.

(v) showed that the currents increased linearly with the v (Figs. S6A and B insets 1, 2), and the logarithmic dependence of  $I_p$  on v had a slope of  $-1.0$  (Figs. S6A and B insets 3), both suggesting a surface-controlled ET for the aptamers. Based on the full-width-at-half maximum of the MB peaks approaching 100 mV, a  $1e^-$  transfer reaction was observed which is consistent with previous reports on aptamer/PEG-modified assays, electrochemistry of intercalated species or attached to dendrimer structures (Álvarez-Martos et al., 2016; Kékedy-Nagy and Ferapontova, 2018; Salimian et al., 2017). Based on the kinetic studies, we expect that the aptamers are vertically oriented on the electrode surface during the electroanalysis, therefore, we can assume that for both surface densities, the ET between the electrode and MB occurred via the aptamer by the generally accepted ET pathway.

Electrochemical aptasensors based on the “on-off” signal change are susceptible to false positives due to non-specific binding, aptamer desorption, deactivation or to any degradation of the SAM layer, and are generally characterized by the decrease of the measured current signal (Liu et al., 2021; Yu et al., 2021a). Based on the small peak shifts observed in the DPVs measured within the clinically relevant range (Fig. 2B), we performed control studies with the aptamer/MC<sub>6</sub>OH-modified electrodes in the absence of  $\Delta^9$ -THC to eliminate the possibility of false positives. As shown in Fig. 3A, over repeated measurements in the presence of 1  $\mu\text{M}$  MB, the  $I_p$  showed no specific decreasing trend (Fig. 3A, inset), in fact, a slight increase was observed, while the normalized  $I_p$  showed a random variation distribution (Fig. 3B). Based on the control studies, the  $I_p$  decrease observed in the presence of  $\Delta^9$ -THC (Fig. 2A and B) are not the result of false positives.

We also studied the specificity of the A-18 aptamer by testing the electrochemical response of the aptasensor platform in the presence of other significant cannabinoid metabolites such as CBN and CBD which makes up to 40% of the extract (Baptista et al., 2002). As shown in Fig. 3C, the presence of 1 nM CBN or CBD does not produce the expected signal decrease as observed in the case of  $\Delta^9$ -THC. In fact, the response exhibited the opposite, showing an increase in the  $I_p$  currents, with CBD producing the highest increase ( $8.9 \pm 0.9 \text{ nA pmol}^{-1} \text{ cm}^2$ ) at the lowest measured concentration (1 nM) from the background current. In the presence of CBN, the  $I_p$  current also showed an increase followed by a negative potential shift (Fig. S7A), while for CBD the  $I_p$  current showed a random variation and a negative potential shift (Fig. S8A) with the increase of the target analyte.

The constructed calibration curves based on the  $I_p$  normalized for the  $I_0$  in response to CBN or CBD concentration did not follow a Langmuir-like affinity binding even though the measured analytical signal showed an opposite trend compared to  $\Delta^9$ -THC response (Figs. S7B and S8B). Data fitting using Eq. (1) resulted in  $K_b$  values of  $0.4 \pm 0.1$  for CBN and  $0.002 \pm 0.0005$  for CBD, with the  $K_d$  of  $1.3 \pm 0.2 \text{ nM}$  and  $0.3 \pm 0.1 \text{ nM}$  for CBN or CBD. As shown in Fig. 3D, both  $K_b$  and  $K_d$  values significantly decrease in the presence of CBN or CBD (compared to THC) and therefore are in agreement with the fluorescence quenching experiment on graphene oxide (Fig. S3). These results show that A-18 aptamer obtained via FRELEX has a high affinity towards  $\Delta^9$ -THC while CBN or CBD does not bind to the aptamer given that these metabolites do not disrupt the

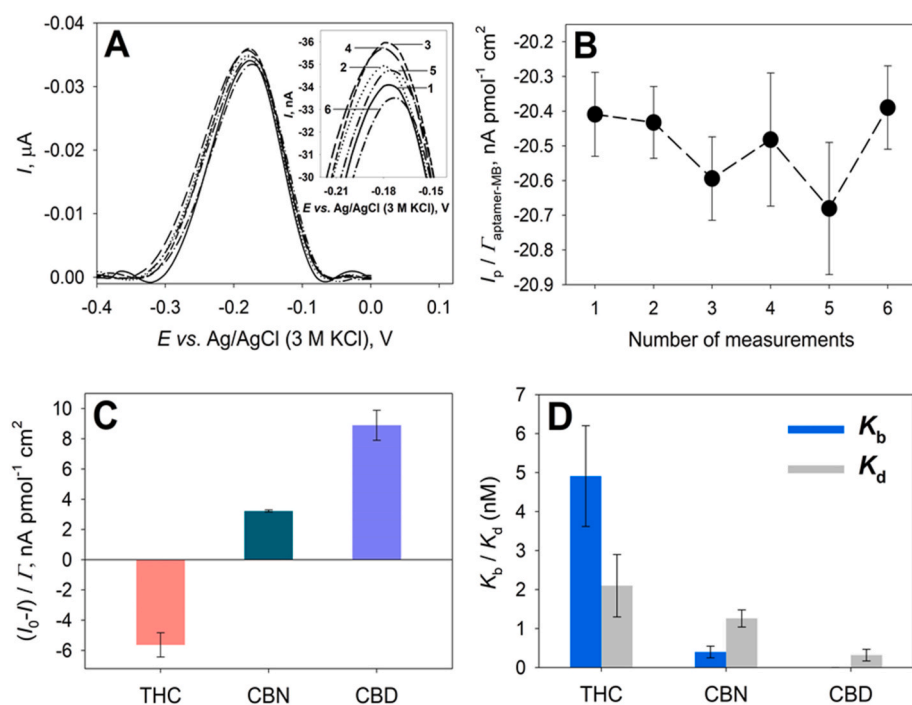


**Fig. 3.** (A) Representative DPVs recorded in 20 mM PBS/150 mM NaCl, pH 7.0 solution containing 1  $\mu\text{M}$  MB with the aptamer/MC<sub>6</sub>OH-modified electrodes in sequence. Inset: the top part of the DPVs representing the sequence from 1 to 6. (B) The normalized  $I_p$  recorded in sequence from 1 to 6 ( $\Gamma_{\text{aptamer-MB}} = 1.8 \pm 0.1 \text{ pmol cm}^{-2}$ ). (C) The normalized  $I_p$  obtained with the 80-nt DNA aptamer in the absence and after exposed to 1 nM of  $\Delta^9$ -THC, CBN or CBD. (D) The  $K_b/K_d$  values obtained from the data fitting of  $\Delta^9$ -THC, CBN or CBD.

aptamer-mediated long-range ET between the electrostatically attracted/intercalated MB and the gold surface.

To verify that the analytical response is due to MB displacement and not from sensor degradation or direct  $\Delta^9$ -THC adsorption on the gold surface through the thiol layer, we performed EIS analysis using MC<sub>6</sub>OH-modified gold disk electrodes in the absence and presence of 100 nM  $\Delta^9$ -THC (Figs. S9A and B). The EIS spectra recorded in the MB/ $\Delta^9$ -THC solutions did not show the expected charge-transfer semicircle,

which demonstrates a minimal distribution of charge and Ohmic contact of the gold surface with the substrates (Fig. S9A). Moreover, based on both the Nyquist and Bode plot (Figs. S9A and B), these show that the trends in the presence of 100 nM  $\Delta^9$ -THC are very similar to the absence of THC case, which suggests that the measured analytical response of the aptasensor is due to MB displacement.

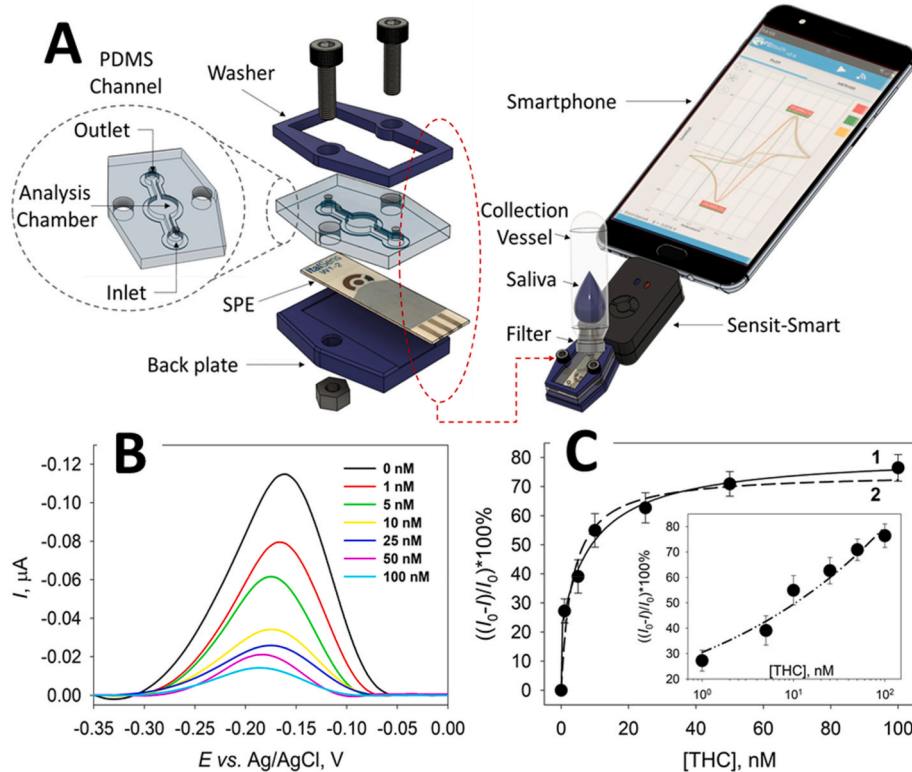


**Fig. 4.** (A) The detailed representation of the fabricated microfluidics chamber for  $\Delta^9$ -THC detection in small volumes with the assembled device (EMMA-Sense). See Video S1 for assembly and operation. (B) Representative DPVs recorded in 20 mM PBS/150 mM NaCl, pH 7.0 solution containing 1  $\mu\text{M}$  MB with the aptamer/MC<sub>6</sub>OH-modified electrodes (black line) before and (colored line) after the additions of 1, 5, 10, 25, 50, and 100 nM of  $\Delta^9$ -THC. (C) Calibration curve of the DPV current signal changes to the background signals in the absence and the presence of various concentrations of  $\Delta^9$ -THC (1–100 nM), where data fitting was performed using (1) the Langmuir adsorption isotherm and (2) the Scatchard model to determine  $K_b$  and  $K_d$ . Inset: the normalized data as of the logarithmic concentration. Surface density:  $\Gamma_{\text{aptamer-MB}} = 4.1 \pm 0.8 \text{ pmol cm}^{-2}$ . To correlate the current change and [THC], a logarithmic fit was used:  $(I_0 - I)/I_0 = ((I_0 - I)/I_0)_0 + a \cdot \log[\Delta^9\text{-THC}]$ , where  $a = 0.416$ .

### 3.2. Detection of $\Delta^9$ -THC in saliva samples using EMMA-sense

As a proof of principle towards point-of-care use of the aptasensor and motivated by the intense interest in developing a low-cost microfluidic platform (Paknahad et al. 2017, 2019; Qiang et al., 2009), we developed an Electrochemical Multipatform Microfluidics Aptamer based Sensor (which we call “EMMA-Sense”) to enable end-users to evaluate  $\Delta^9$ -THC in saliva via electrochemistry using their cellphone. Fig. 4A shows the microfluidic chamber consisting of a 3D-printed fastening hardware (mounting washer and back plate), which applies pressure to form a liquid-tight seal between a PDMS channel layer and the commercially available SPE. For aptamer integration with the SPE, we used the high aptamer surface coverage with the microfluidics device (based on Table 1). As with similar microfluidics electrochemical detection (Dryden et al., 2013; Lee et al., 2017; Salahandish et al., 2022), each electrode was connected to a contact pad and left exposed (i. e. not covered by the PDMS), such that it can be connected to our hand-held potentiostat and cellphone, see Fig. 4A and Video S1.

The EMMA-Sense was validated by obtaining representative DPVs (see Fig. 4B) using small sample volumes (60  $\mu$ L) for various concentrations (0–100 nM) of  $\Delta^9$ -THC in PBS and MB. Each curve shows a gradual decrease upon the addition of  $\Delta^9$ -THC in the clinically relevant concentration range. Moreover, the device could clearly detect the presence of 1 nM of  $\Delta^9$ -THC in PBS which showed a 1.4-fold decrease (similar to what we obtained previously with the conventional three-electrode cell configuration, see above). The calibration curves constructed based on the DPV responses and fitted using Eq. (1) and Eq. (2), see Fig. 4C, showed a value for  $K_b = 3.8 \pm 0.5$  and  $K_d = 2.2 \pm 0.4$  nM, with a LOD of 1 nM, which is 6-fold lower than the regulatory limit set by multiple countries (Gjerde and Verstraete, 2011; Johnson et al., 2022; Vindenes et al., 2012). The performance of our sensor platform is comparable to the conventional gold-disk electrode in a three-electrode electrochemical system (see Table 1).

Next, we applied the new EMMA-Sense platform to study the aptasensor performance in presence of raw saliva (individual #4, see participant characteristics, Table S1), and diluted the raw saliva with 20 mM PBS/150 mM NaCl/1  $\mu$ M MB (pH 7.0) and spiked  $\Delta^9$ -THC to 50% followed by measuring the signals after 1 min. The  $I_p$  of the observed

DPVs showed no clear trend for various spiked  $\Delta^9$ -THC (Fig. S10A), therefore, we further diluted the saliva to 10%, where the  $I_p$  signals (Fig. S10B) showed decreasing trend upon the addition of  $\Delta^9$ -THC (10–50 nM) with Langmuir-like affinity binding (see Fig. 5A). The saliva displayed a major impact on the aptasensor performance by exhibiting a higher  $K_b$  of  $51 \pm 8.5$  and  $K_d$  of  $58 \pm 8.5$  nM, and a LOD of 10 nM. Consequently, we applied a 10 kDa size exclusion centrifugation column to filter out the major proteins (e.g., mucins, proline-rich proteins (PRPs),  $\alpha$ -amylase, secretory IgA, cystatins or statherin) that could negatively influence the aptasensor performance (Schenkels et al., 1995). The protein concentration in saliva before and after filtration was estimated by measuring the UV absorbance at  $\sim$ 280 nm and showed a decrease for the filtered sample (Fig. S11) suggesting that some proteins that were affecting our signal have been removed.

In addition, we tested the repeatability and reproducibility of our sensor by recording DPVs from 50% diluted and filtered saliva collected from four adult volunteers (see participant characteristics, Table S1) in the absence and in the presence of 5 nM  $\Delta^9$ -THC. As shown in Fig. S12, there is a decrease in the measured cathodic DPV currents when  $\Delta^9$ -THC was present. The normalized  $I_p$  for the background also showed a decrease between 9.1% and 9.7% in the analytical signal (see Fig. 5B and Table S3), showing good repeatability based on the minimal coefficient of variance ( $<0.7\%$ ) between the participants (see Table S3). Using an one-way variance analysis (ANOVA), there is no significant difference between the four test subjects [ $p = 0.65 < 0.05$  and  $F < F_{crit}$  ( $0.571 < 4.066$ )], suggesting the aptasensor gave reproducible signals for different saliva samples. Furthermore, the EMMA-Sense platform was able to successfully distinguish the presence of 5 nM  $\Delta^9$ -THC in human saliva, which is lower than the cut-off values of 6.5–32 nM generally established by countries for driving under the influence (Ortega et al., 2022).

Moving towards a rapid diagnostic for  $\Delta^9$ -THC, we evaluated the storage stability of the EMMA-Sense platform by storing the aptamer-modified electrodes in a dry state at 4  $^{\circ}$ C. Previous studies showed that aptamer-modified electrodes stored in buffer solution tend to accelerate desorption of thiols from the gold layer and leads to faster degradation in the presence of  $O_2$  and  $H_2O$  (Salimian et al., 2017). The aptasensor showed a decrease of  $10.8 \pm 1.2\%$  in the normalized  $I_p$  for

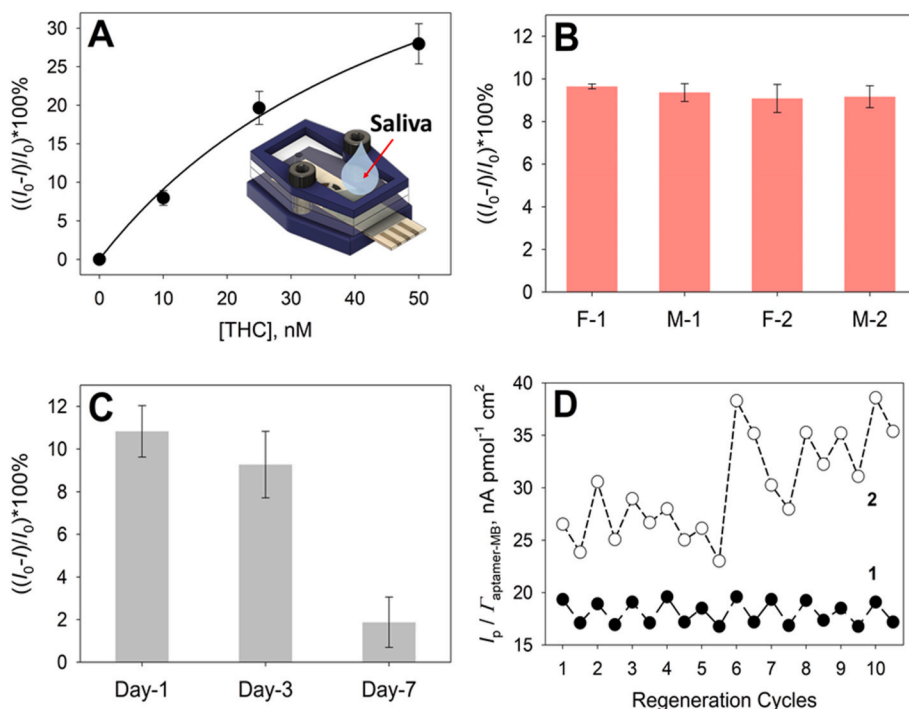


**Fig. 5.** (A) Dependences of the DPV current signal changes to the background signals in the absence and the presence of various concentrations of  $\Delta^9$ -THC (10–50 nM) in 90% diluted raw human saliva. To correlate the current change and [THC], a logarithmic fit was used:  $(I_0 - I)/I_0 = ((I_0 - I)/I_0)_0 + a \cdot \log[\Delta^9\text{-THC}]$ , where  $a = 0.483$ . (B) The normalized  $I_p$  signal intensities to the background measured in 50% filtered human saliva containing PBS/1  $\mu$ M MB in the presence of 5 nM  $\Delta^9$ -THC. The reported values represent the average results from three separate experiments ( $n = 3$ ), and the error bars represent the standard deviation. Surface density:  $\Gamma_{\text{aptamer-MB}} = 3.8 \pm 0.4$  pmol  $\text{cm}^{-2}$ . (C) Storage stability of the EMMA-Sense based on the normalized  $I_p$  signal intensities to the background measured in 50% filtered human saliva containing PBS/1  $\mu$ M MB in the presence of 5 nM  $\Delta^9$ -THC. (D) Regeneration of the (1) freshly prepared and (2) after stored for 3 days EMMA-Sense based on the  $I_p$  signal intensities normalized for the  $\Gamma_{\text{aptamer-MB}}$  recorded in the absence/presence of 5 nM  $\Delta^9$ -THC by rinsing with PBS for 1 min.

the background with freshly prepared electrodes, while after 3 days of storage, the analytical signal decrease was similar to the freshly prepared electrodes ( $9.3 \pm 1.5\%$ ; see Fig. 5C). These values are in good agreement with the measurements obtained with the freshly prepared electrode in four different saliva samples (see Fig. 5B). However, the aptasensor showed only a  $1.9 \pm 1.2\%$  decrease in the analytical signal after one week storage in the presence of 5 nM  $\Delta^9$ -THC (see Fig. 5C), which suggests a thiol layer degradation or aptamer desorption from the gold surface.

Finally, we also studied the regeneration (or reusability) capability of the aptasensor platform. As shown in Fig. 5D, EMMA-Sense showed good regeneration up to 10 cycles with the freshly prepared electrode after washing the sensor with PBS for 1 min between the cycle of challenge with 5 nM  $\Delta^9$ -THC ( $\sim 1\%$  CV; see Table S4). The reusability of  $\Delta^9$ -THC aptasensor was significantly affected after 3 days of storage in dry conditions, such that it could be regenerated up to 5 cycles (see Fig. 5D;  $\sim 5\%$  CV) but showed poor regenerative capability after 10 cycles ( $>15\%$  CV). The regeneration of the aptasensor was exacerbated after 7 days of storage (see Fig. S13;  $\sim 10$ – $14\%$  CV) suggesting the device is not suitable for week-long storage. The behavior has been reported previously (Salimian et al., 2017), which is likely caused by aptamer/thiol layer desorption during the cycles such that the buffer could be removing the aptamer from the gold-surface as the thiol bond dissociates over time.

Compared to other rapid detection methods for the detection of  $\Delta^9$ -THC (see Table S5), the EMMA-Sense shows several advantages, for example, rapid analysis, portability, and a low limit of detection that allows for linear performance in the clinically relevant range. Although this technique was carried out to only detect  $\Delta^9$ -THC, it would be straightforward to expand such a system towards multiplexed sensing enabling multiple cannabinoids could be detected simultaneously such that the collection of measurements will provide a more accurate assessment for cannabis impairment. We propose that the new methods described here may be particularly useful for applications involving cannabinoid detection in the medical, athletic, and law enforcement contexts.

#### 4. Conclusions

In this work, we propose a novel, signal “on-off”, cost-effective, rapid (1 min) electrochemical aptasensor for the detection of  $\Delta^9$ -THC in human saliva using label-free 80-nt  $\Delta^9$ -THC specific aptamer sequence obtained with FRELEX via DPV in conjunction with a PDMS-based microfluidic cartridge setup. The aptasensor exploits the  $\Delta^9$ -THC's aptamer binding affinity which displaces the soluble redox indicator (MB) and reduces the ET at the working electrode. In a three-electrode cell system, the aptasensor was able to detect the presence of 1 nM of  $\Delta^9$ -THC in PBS, while the sensitivity, and the  $K_b/K_d$  both showed dependence on the aptamer surface coverage. The aptamer showed a great affinity towards  $\Delta^9$ -THC which was reflected in the  $K_b$  decrease by a 12-fold for CBN and 2557-fold for CBD, respectively. Measurements performed in small volume samples ( $\sim 60$   $\mu$ L) with the aptamer modified gold-SPE combined with the microfluidic cartridge setup showed a similar LOD of 1 nM in PBS. On the other hand, the presence of 10% diluted raw human saliva had a detrimental effect on the aptasensor performance which manifested in a 10-fold increase of the LOD due to interfering elements. Pretreatment of saliva by size exclusion filtration improved the LOD to 5 nM of  $\Delta^9$ -THC which is lower than the concentrations associated with impairment (6.5–32 nM) and also increased the tested saliva volume to 50%. The aptasensor showed a good storage capability up to 3 days when stored in dry conditions at 4 °C, however, the reusability significantly dropped from 10 cycles (freshly prepared) to 5 cycles. The results clearly demonstrate the feasibility regarding the applicability of the electrochemical aptasensor equipped with the microfluidics chamber towards a rapid point-of-care platform for the detection of  $\Delta^9$ -THC in saliva.

#### CRedit authorship contribution statement

**László Kékedy-Nagy:** Conceptualization, Methodology, Validation, Formal analysis, Investigation, Visualization, Writing – original draft, Writing – review & editing. **James M. Perry:** Conceptualization, Methodology, Visualization, Writing – original draft, Writing – review & editing. **Samuel R. Little:** Investigation, Writing – review & editing. **Oriol Y. Llorens:** Conceptualization, Methodology, Writing – review & editing. **Steve.C.C. Shih:** Conceptualization, Methodology, Resources, Writing – original draft, Writing – review & editing, Supervision, Project administration, Funding acquisition, All authors reviewed and edited the manuscript before submission.

#### Declaration of competing interest

The authors declare that they have no known competing financial interests or personal relationships that could have appeared to influence the work reported in this paper.

#### Data availability

Data will be made available on request.

#### Acknowledgements

We would like to thank Dr. Gregory Penner from Neoventures for his help with the FRELEX and analysis. We thank the Natural Sciences and Engineering Research Council (NSERC) (including the SynBioApps CREATE program), the Fonds de Recherche Nature et Technologies (FRQNT), MEDTEQ+, the Canadian Foundation of Innovation (CFI), and Mitacs for funding. LKN thanks Mitacs for an Accelerate PDF scholarship. SRL thank NSERC for a CGS scholarship and Concordia University Department of Electrical and Computer Engineering for FRS Funding. SCCS thanks Concordia for a University Research Chair.

#### Appendix A. Supplementary data

Supplementary data to this article can be found online at <https://doi.org/10.1016/j.bios.2022.114998>.

#### References

- Álvarez-Martos, I., Kartashov, A., Ferapontova, E.E., 2016. Electron transfer in methylene-blue-labeled G3 dendrimers tethered to gold. *Chemelectrochem* 3 (12), 2270–2280.
- Balbino, M.A., de Menezes, M.M.T., Eleotério, I.C., Saczk, A.A., Okumura, L.L., Tristão, H.M., de Oliveira, M.F., 2012. Voltammetric determination of  $\Delta^9$ -THC in glassy carbon electrode: an important contribution to forensic electroanalysis. *Forensic Sci. Int.* 221 (1–3), 29–32.
- Balbino, M.A., Ojye, É.N., Ribeiro, M.F.M., Júnior, J.W.C., Eleotério, I.C., Ipólito, A.J., de Oliveira, M.F., 2016. Use of screen-printed electrodes for quantification of cocaine and  $\Delta^9$ -THC: adaption to portable systems for forensic purposes. *J. Solid State Electrochem.* 20 (9), 2435–2443.
- Baptista, M.J., Monsanto, P.V., Marques, E.G.P., Bermejo, A., Ávila, S., Castanheira, A. M., Margalho, C., Barroso, M., Vieira, D.N., 2002. Hair analysis for  $\Delta^9$ -THC,  $\Delta^9$ -THC-COOH, CBN and CBD, by GC/MS-EI: comparison with GC/MS-NCI for  $\Delta^9$ -THC-COOH. *Forensic Sci. Int.* 128 (1–2), 66–78.
- Bueno, P.R., Davis, J.J., 2014. Elucidating redox-level dispersion and local dielectric effects within electroactive molecular films. *Anal. Chem.* 86 (4), 1997–2004.
- Campos, R., Kotlyar, A., Ferapontova, E.E., 2014. DNA-mediated electron transfer in DNA duplexes tethered to gold electrodes via phosphorothioated dA tags. *Langmuir* 30 (40), 11853–11857.
- Connors, N., Kosnett, M.J., Kulig, K., Nelson, L.S., Stolbach, A.I., 2020. ACMT position statement: interpretation of urine for tetrahydrocannabinol metabolites. *J. Med. Toxicol.* 16 (2), 240–242.
- Darzi, E.R., Garg, N.K., 2020. Electrochemical oxidation of  $\Delta^9$ -tetrahydrocannabinol: a simple strategy for marijuana detection. *Org. Lett.* 22 (10), 3951–3955.
- De Rycke, E., Stove, C., Dubruel, P., De Saeger, S., Beloglazova, N., 2020. Recent developments in electrochemical detection of illicit drugs in diverse matrices. *Biosens. Bioelectron.* 169, 112579.
- Degenhardt, L., Tennant, C., Gilmour, S., Schofield, D., Nash, L., Hall, W., McKay, D., 2007. The temporal dynamics of relationships between cannabis, psychosis and

- depression among young adults with psychotic disorders: findings from a 10-month prospective study. *Psychol. Med.* 37 (7), 927–934.
- Dryden, M.D.M., Rackus, D.D.G., Shamsi, M.H., Wheeler, A.R., 2013. Integrated digital microfluidic platform for voltammetric analysis. *Anal. Chem.* 85 (18), 8809–8816.
- Farjami, E., Clima, L., Gothelf, K.V., Ferapontova, E.E., 2010. DNA interactions with a methylene blue redox indicator depend on the DNA length and are sequence specific. *Analyst* 135 (6), 1443–1448.
- Ferapontova, E.E., Gothelf, K.V., 2009. Effect of serum on an RNA aptamer-based electrochemical sensor for theophylline. *Langmuir* 25 (8), 4279–4283.
- Gjerde, H., Verstraete, A.G., 2011. Estimating equivalent cutoff thresholds for drugs in blood and oral fluid using prevalence regression: a study of tetrahydrocannabinol and amphetamine. *Forensic Sci. Int.* 212 (1–3), e26–e30.
- Goodwin, A., Banks, C.E., Compton, R.G., 2006. Graphite micropowder modified with 4-Amino-2, 6-diphenylphenol supported on basal plane pyrolytic graphite electrodes: micro sensing platforms for the indirect electrochemical detection of  $\Delta^9$ -Tetrahydrocannabinol in saliva. *Electroanalysis* 18 (11), 1063–1067.
- Grotenhermen, F., 2003. Pharmacokinetics and pharmacodynamics of cannabinoids. *Clin. Pharmacokinet.* 42 (4), 327–360.
- Hall, W., Degenhardt, L., 2008. Cannabis use and the risk of developing a psychotic disorder. *World Psychiatr.* 7 (2), 68.
- Howard, J., Osborne, J., 2020. Cannabis and work: need for more research. *Am. J. Ind. Med.* 63 (11), 963–972.
- Jacobsen, M.F., Ferapontova, E.E., Gothelf, K.V., 2009. Synthesis and electrochemical studies of an anthraquinone-conjugated nucleoside and derived oligonucleotides. *Org. Biomol. Chem.* 7 (5), 905–908.
- Jarczewska, M., Kékedy-Nagy, L., Nielsen, J.S., Campos, R., Kjem, J., Malinowska, E., Ferapontova, E.E., 2015. Electroanalysis of pM-levels of urokinase plasminogen activator in serum by phosphorothioated RNA aptamer. *Analyst* 140 (11), 3794–3802.
- Johnson, O.E., Miskelly, G.M., Rindelaub, J.D., 2022. Testing for cannabis intoxication: current issues and latest advancements. *WIREs Forensic Sci* 4 (4), e1450.
- Kékedy-Nagy, L., Ferapontova, E.E., 2018. Sequence-specific electron transfer mediated by DNA duplexes attached to gold through the alkanethiol linker. *J. Phys. Chem. B* 122 (44), 10077–10085.
- Kékedy-Nagy, L., Shipovskov, S., Ferapontova, E.E., 2016. Effect of a dual charge on the DNA-conjugated redox probe on DNA sensing by short hairpin beacons tethered to gold electrodes. *Anal. Chem.* 88 (16), 7984–7990.
- Kelley, S.O., Barton, J.K., Jackson, N.M., Hill, M.G., 1997. Electrochemistry of methylene blue bound to a DNA-modified electrode. *Bioconjugate Chem.* 8 (1), 31–37.
- Kennedy, M., 2022. Cannabis, cannabidiol and tetrahydrocannabinol in sport: an overview. *Intern. Med.* J. 52, 1471–1477.
- Khalili, P., Nadimi, A.E., Baradaran, H.R., Janani, L., Rahimi-Movaghar, A., Rajabi, Z., Rahmani, A., Hojati, Z., Khalagi, K., Motevalian, S.A., 2021. Validity of self-reported substance use: research setting versus primary health care setting. *Subst. Abuse Treat. Prev. Pol.* 16 (1), 1–13.
- Klimuntowski, M., Alam, M.M., Singh, G., Howlader, M.M.R., 2020. Electrochemical sensing of cannabinoids in biofluids: a noninvasive tool for drug detection. *ACS Sens.* 5 (3), 620–636.
- Lee, G.H., Lee, J.K., Kim, J.H., Choi, H.S., Kim, J., Lee, S.H., Lee, H.Y., 2017. Single microfluidic electrochemical sensor system for simultaneous multi-pulmonary hypertension biomarker analyses. *Sci. Rep.* 7 (7545), 1–8.
- Liu, Y., Canoura, J., Alkhamis, O., Xiao, Y., 2021. Immobilization strategies for enhancing sensitivity of electrochemical aptamer-based sensors. *ACS Appl. Mater. Interfaces* 13 (8), 9491–9499.
- Majak, D., Fan, J., Kang, S., Gupta, M., 2021. Delta-9-tetrahydrocannabinol ( $\Delta^9$ -THC) sensing using an aerosol jet printed organic electrochemical transistor (OECT). *J. Mater. Chem. B* 9 (8), 2107–2117.
- Mirzaei, H., O'Brien, A., Tasnim, N., Ravishankara, A., Tahmooressi, H., Hoorfar, M., 2020. Topical review on monitoring tetrahydrocannabinol in breath. *J. Breath Res.* 14 (3), 034002.
- Nafisi, S., Saboury, A.A., Keramat, N., Neault, J.-F., Tajmir-Riahi, H.-A., 2007. Stability and structural features of DNA intercalation with ethidium bromide, acridine orange and methylene blue. *J. Mol. Struct.* 827 (1–3), 35–43.
- Nissim, R., Compton, R.G., 2015. Absorptive stripping voltammetry for cannabis detection. *Chem. Cent. J.* 9 (1), 1–7.
- Novak, I., Mlakar, M., Komorsky-Lovrić, Š., 2013. Voltammetry of immobilized particles of cannabinoids. *Electroanalysis* 25 (12), 2631–2636.
- Ortega, G.A., Ahmed, S.R., Tuteja, S.K., Srinivasan, S., Rajabzadeh, A.R., 2022. A biomolecule-free electrochemical sensing approach based on a novel electrode modification technique: detection of ultra-low concentration of  $\Delta^9$ -tetrahydrocannabinol in saliva by turning a sample analyte into a sensor analyte. *Talanta* 236, 122863.
- Paknahad, M., Bachhal, J.S., Ahmadi, A., Hoorfar, M., 2017. Characterization of channel coating and dimensions of microfluidic-based gas detectors. *Sensor. Actuator. B Chem.* 241, 55–64.
- Paknahad, M., McIntosh, C., Hoorfar, M., 2019. Selective detection of volatile organic compounds in microfluidic gas detectors based on “like dissolves like.”. *Sci. Rep.* 9 (1), 1–11.
- Papafotiou, K., Carter, J.D., Stough, C., 2005. An evaluation of the sensitivity of the Standardised Field Sobriety Tests (SFSTs) to detect impairment due to marijuana intoxication. *Psychopharmacology* 180 (1), 107–114.
- Penner, G., 2019. Method for the Selection of Aptamers for Unbound Targets. NeoVentures Biotechnology Inc.
- Qiang, W., Zhai, C., Lei, J., Song, C., Zhang, D., Sheng, J., Ju, H., 2009. Disposable microfluidic device with ultraviolet detection for highly resolved screening of illicit drugs. *Analyst* 134 (9), 1834–1839.
- Renaud-Young, M., Mayall, R.M., Salehi, V., Golezdzinski, M., Comeau, F.J.E., MacCallum, J.L., Birss, V.I., 2019. Development of an ultra-sensitive electrochemical sensor for  $\Delta^9$ -tetrahydrocannabinol (THC) and its metabolites using carbon paper electrodes. *Electrochim. Acta* 307, 351–359.
- Salahandish, R., Hassani, M., Zare, A., Haghayegh, F., Sanati-Nezhad, A., 2022. Autonomous electrochemical biosensing of glial fibrillary acidic protein for point-of-care detection of central nervous system injuries. *Lab Chip* 22 (8), 1542–1555.
- Salimian, R., Kékedy-Nagy, L., Ferapontova, E.E., 2017. Specific picomolar detection of a breast cancer biomarker HER-2/neu protein in serum: electrocatalytically amplified electroanalysis by the aptamer/PEG-modified electrode. *Chemelectrochem* 4 (4), 872–879.
- Saugy, M., Avois, L., Saudan, C., Robinson, N., Giroud, C., Mangin, P., Dvorak, J., 2006. Cannabis and sport. *Br. J. Sports Med.* 40 (Suppl. 1), i13–i15.
- Schenkels, L.C., Veerman, E., Nieuw Amerongen, A.V., 1995. Biochemical composition of human saliva in relation to other mucosal fluids. *Crit. Rev. Oral Biol. Med.* 6 (2), 161–175.
- Shanmugam, S.T., Trashin, S., De Wael, K., 2020. Gold-sputtered microelectrodes with built-in gold reference and counter electrodes for electrochemical DNA detection. *Analyst* 145 (23), 7646–7653.
- Stojanovic, M.N., De Prada, P., Landry, D.W., 2001. Aptamer-based folding fluorescent sensor for cocaine. *J. Am. Chem. Soc.* 123 (21), 4928–4931.
- Teymourian, H., Parrilla, M., Sempionatto, J.R., Montiel, N.F., Barfidokht, A., Van Echelpoel, R., De Wael, K., Wang, J., 2020. Wearable electrochemical sensors for the monitoring and screening of drugs. *ACS Sens.* 5 (9), 2679–2700.
- Trasatti, S., Petrii, O.A., 1991. Real surface area measurements in electrochemistry. *Pure Appl. Chem.* 63 (5), 711–734.
- Vemuri, V.K., Makriyannis, A., 2015. Medicinal chemistry of cannabinoids. *Clin. Pharmacol. Ther.* 97 (6), 553–558.
- Vindenes, V., Jordbru, D., Knapskog, A.-B., Kvan, E., Mathisrud, G., Slørdal, L., Mørland, J., 2012. Impairment based legislative limits for driving under the influence of non-alcohol drugs in Norway. *Forensic Sci. Int.* 219 (1–3), 1–11.
- Yoo, H., Jo, H., Oh, S.S., 2020. Detection and beyond: challenges and advances in aptamer-based biosensors. *Mater. Adv.* 1 (8), 2663–2687.
- Yu, H., Alkhamis, O., Canoura, J., Liu, Y., Xiao, Y., 2021a. Advances and challenges in small-molecule DNA aptamer isolation, characterization, and sensor development. *Angew. Chem. Int. Ed.* 60 (31), 16800–16823.
- Yu, H., Lee, H., Cheong, J., Woo, S.W., Oh, J., Oh, H.-K., Lee, J.-H., Zheng, H., Castro, C. M., Yoo, Y.-E., 2021b. A rapid assay provides on-site quantification of tetrahydrocannabinol in oral fluid. *Sci. Transl. Med.* 13 (616), eabe2352.
- Yu, H., Luo, Y., Alkhamis, O., Canoura, J., Yu, B., Xiao, Y., 2021c. Isolation of natural DNA aptamers for challenging small-molecule targets, cannabinoids. *Anal. Chem.* 93 (6), 3172–3180.
- Zhang, Y., You, Z., Hou, C., Liu, L., Xiao, A., 2021. An electrochemical sensor based on amino magnetic nanoparticle-decorated graphene for detection of cannabidiol. *Nanomaterials* 11 (9), 2227.
- Zheng, X., Zhang, F., Wang, K., Zhang, W., Li, Y., Sun, Y., Sun, X., Li, C., Dong, B., Wang, L., 2021. Smart biosensors and intelligent devices for salivary biomarker detection. *Trends Anal. Chem.* 140, 116281.